Acta Cryst. (1973). A**29**, 138

*n*B-eam Lattice Images. III. Upper Limits of Ionicity in $W_4Nb_{26}O_{77}$

BY G. R. ANSTIS

Department of Mathematical Physics, University of Adelaide, South Australia, Australia,

D. F. LYNCH, A. F. MOODIE

Division of Chemical Physics, CSIRO, P. O. Box 160, *Clayton, Victoria, Australia* 3168

AND M. A. O'KEEFE

Division of Tribophysics, CSIRO, University of Melbourne, Parkville, Victoria, Australia 3052

(*Received* 23 *June* 1972; *accepted 3 October* 1972)

The scattering factor for electrons is sensitive to differences in atomic bonding at low values of sin θ/λ. These differences will influence the amplitudes and phases of low-order beams of electrons diffracted from crystals with large unit cells. The experimental intensities of these beams, and contrast in the corresponding lattice images, can be used to derive upper limits for the charges on constituent ions, provided the associated *n*-beam dynamical calculations are carried out with sufficient precision. It is shown that, in $W_4Nb_{26}O_{77}$, the atoms can be only partially ionized, and the bonding must have some covalent character.

Introduction

In parts I (Allpress, Hewat, Moodie & Sanders, 1972) and II (Lynch & O'Keefe, 1972) of the above running title, it was shown that the Cowley & Moodie (1957) theory of *n*-beam dynamical scattering can be used to calculate the complex amplitudes of the diffracted electron beams from crystals with large unit cells, and the Cowley & Moodie (1960) Fourier-image theory used to construct crystal-lattice images from the calculated diffracted beam amplitudes. Both the calculated diffracted beam intensities and the calculated images agreed with experimental results.

A number of effects are specific to large unit cells of the type considered in the present investigation; two of these which are of particular importance at conventional accelerating voltages (say in the region of 100 kV) are the large number of reciprocal lattice points that lie on an effectively planar area of the Ewald sphere, and the small scattering angles of the first few orders of diffraction. The first factor suggests that interpretation in terms of charge density (Cowley & Moodie, 1960) may frequently serve, at least as a guide, in interpretation of the structure, since the thin-phase-grating approximation (Moodie, 1972) holds when the excitation errors are effectively zero. This, in turn, permits interpretation of the intensity distribution in the image at small defect of focus in terms of charge density (Cowley & Moodie, 1960). As at small angles the scattering of electrons is a sensitive function of the bonding in the crystal, the second factor suggests that quantitative information on bonding should be obtainable from some images. In fact, it will be shown that both types of information can be obtained by noting the dependence of the images on thickness.

For thin crystals, the charge-density approximation holds to some level of resolution. Inner reflexions alter the image in accordance with the rearrangement of electrons due to bonding, but this is a very small effect. Thus, from the point of view of structure determination by the direct observation of sufficiently thin crystals, the image is completely insensitive to the models used for the constituent atoms. Similarly, in a rigorous calculation aimed only at the elucidation of structure from images of thin crystals, any plausible atomic scattering factor can be used, for instance that for a neutral atom. As the thickness increases, the charge-density approximation fails (Cowley & Moodie, 1960), and the images depend increasingly on bonding and, hence, on the models used for the constituent atoms. At these thicknesses, of course, the images do not represent the structure directly, although they are equally detailed, and reflect the crystal symmetries (Cowley & Moodie, 1959; Gjønnes & Moodie, 1965).

The effect of ionization on atomic scattering factors for electrons is very much larger than for X-rays, and is particularly apparent at small values of sin θ/λ. For example, Fig. 1 shows the scattering curves (Cromer & Waber, 1965) for the isolated tungsten atom, in both neutral and fully ionized states, calculated for X-rays (*a*) and electrons (*b*). As suggested by Cowley (1953), the electron scattering-factor graphs indicate that the intensities of diffracted electron beams, suitably interpreted dynamically, should provide useful information on ionicity.

In the present calculation three types of form factors were tested against experiment. First, the usual model for an ionic crystal was used, that is, one with isolated-ion form factors. This implies pure ionic bonding with no overlap of charge density but extensive overlap of potential. Second, a model with ionicity

was used, that is the field of the ions is assumed to affect the electron distribution in a way which results in reduction of the effective charge of the ion from the valency value (Pauling, 1960). In this case there is still no overlap of charge density. Finally, it was found necessary to refine the ionicity model by introducing changes in the form factor which led to some small amount of overlap in the charge distribution, in other words, introduced some covalent character into the bonds.

Choice of material

In order to exploit the sensitivity to ionicity at low values of $\sin\theta/\lambda$, our initial experiments have been made using the complex oxide – $W_4Nb_{26}O_{77}$. This material has two axes greater than 2 nm in length, and the points marked × in Fig. 1 indicate the values of $\sin\theta/\lambda$ for the first seven 00*l* reflexions. The structure of the oxide was determined by Andersson, Mumme & Wadsley (1966).

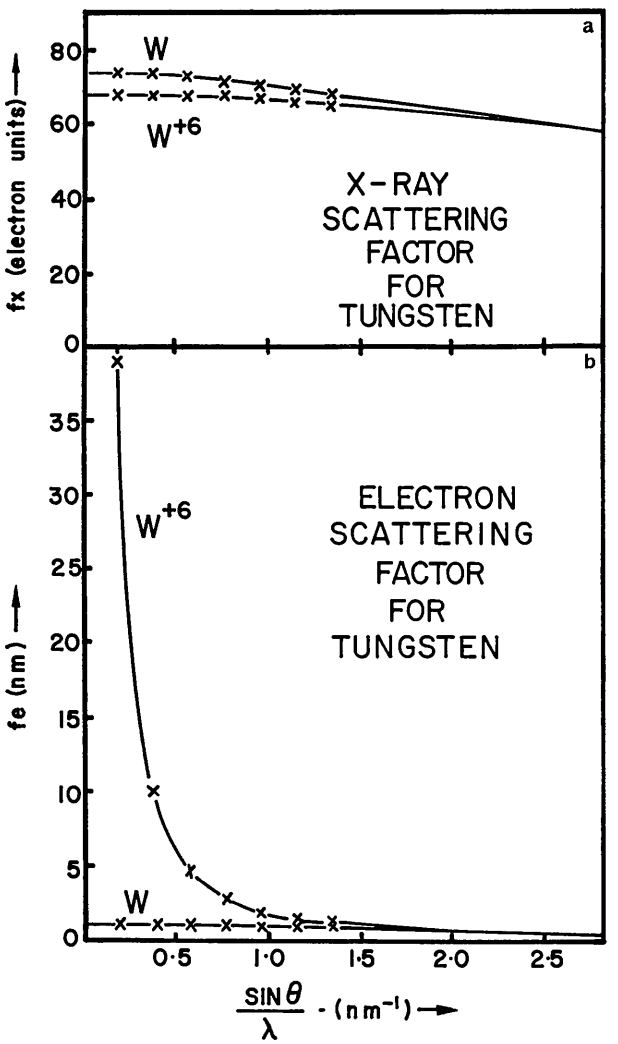

Fig. 1. X-ray (*a*) and electron (*b*) scattering factors for neutral and fully (6+) ionized tungsten atoms. The points × indicate the values of $\sin\theta/\lambda$ for the first seven 00*l* reflexions in $W_4Nb_{26}O_{77}$, *i.e.* where the curves were sampled in the course of the calculations.

Experimental

Samples of $W_4Nb_{26}O_{77}$ were provided by the late Dr A. D. Wadsley. They were finely ground and dispersed on carbon-coated grids for examination in an electron microscope. Previous work has shown that the grinding technique for specimen preparation did not alter or deform the material in any way (Allpress, Sanders & Wadsley, 1969; Allpress & Roth, 1971).

Areas of thin fragments which appeared to be of nearly uniform thickness were selected, and were oriented so that the 00*l* systematic set of reflexions was visible in the electron diffraction patterns; two sets of measurements were then made. In the first set, diffraction patterns were recorded using focused illumination, so that each spot in the pattern appeared as a disc, within which the angle of incidence varied by the amount of divergence in the incident beam. The second set of measurements consisted of a through-focus series of lattice images, recorded in the 00*l* systematics orientation, with 11 beams allowed through the objective aperture to form the image (Allpress, Hewat, Moodie & Sanders, 1972).

Calculations

Multislice dynamical calculations of a set of 00*l* systematics reflexions for $W_4Nb_{26}O_{77}$ based on the structural data of Andersson *et al.* (1966) were carried out using the one-dimensional systematics multislice and the two-dimensional multislice approximations*(Lynch & O'Keefe, 1972). The electron scattering factors were calculated from the Dirac–Slater X-ray scattering factors published by Cromer & Waber (1965). Scattering calculations were carried out for:

(i) neutral atoms;
(ii) partially ionized $W^{+0.8}$, $Nb^{+0.8}$, $O^{-0.4}$ and $W^{+1.4}$, $Nb^{+1.8}$, $O^{-0.7}$;

and

(iii) fully ionized W^{+6}, Nb^{+5}, O^{-2} atoms.

Partial ionization or ionicity (Pauling, 1960), is the well known method of representing the effect of the overlap potential on neighbouring ions in the case when there is *no* overlap of the charge distribution of the neighbouring ions.

Electron scattering factors for the partially ionized species were derived by linear interpolation between the neutral and fully ionized curves. Structure amplitudes for the various models are displayed in Table 1.

* Multislice calculations were made for 29 beams in the systematics case and 435 beams in the two-dimensional case.

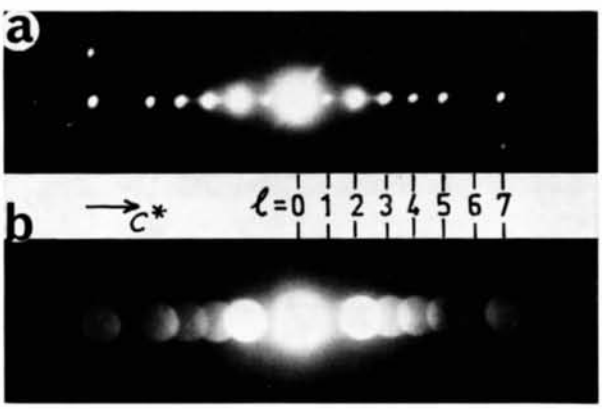

Fig. 2. Experimental systematics (00*l*) electron diffraction pattern from a fragment of $W_4Nb_{26}O_{77}$ of approximately 30 nm thickness (Allpress *et al.*, 1972): (*a*) point pattern; (*b*) disc pattern formed by defocusing the condenser lens.

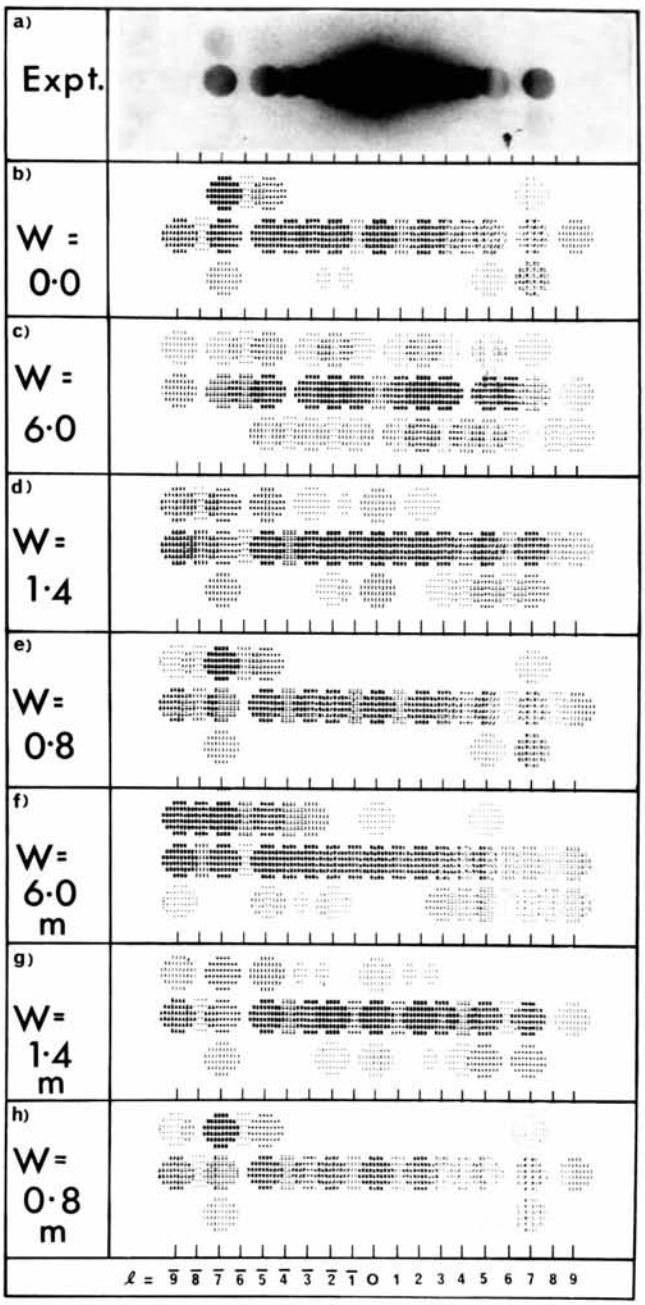

Fig. 6. Diffracted *h*0*l* electron-beam intensities (calculated using the two-dimensional multislice method) for a crystal thickness of 30 nm and a crystal tilt of 0·1 rad. about the c^* axis whilst maintaining equal 00*l* and 00$\bar{l}$ excitation. (*a*) Experimental diffraction pattern; (*b*) $W_4Nb_{26}O_{77}$ (neutral atoms); (*c*) $W_4^{6+}Nb_{26}^{5+}O_{77}^{2-}$ (fully ionized atoms); (*d*) $W_4^{1\cdot4+}Nb_{26}^{1\cdot8+}O_{77}^{0\cdot7-}$; (*e*) $W_4^{0\cdot8+}Nb_{27}^{1\cdot0+}O_{77}^{0\cdot7-}$; (*f*) $W_4^{6+}Nb_{26}^{5+}O_{77}^{2-}$ (modified atom scattering factors), (*g*) $W_4^{1\cdot4+}Nb_{26}^{1\cdot8+}O_{77}^{0\cdot7-}$ (modified atom scattering factors); (*h*) $W_4^{0\cdot8+}Nb_{26}^{1\cdot0+}O_{77}^{0\cdot4-}$ (modified atom scattering factors).

[*To face p.* 139

Lattice images were computed by Fourier summing the complex amplitudes of the diffracted beams produced by the electron-scattering calculations (Lynch & O'Keefe, 1972).

Results

Fig. 2 shows a typical 00*l* electron diffraction pattern from a fragment of $W_4Nb_{26}O_{77}$ (Allpress *et al.*, 1972). The exact thickness of the fragments was difficult to estimate, but experience with similar samples containing Wadsley defects (Allpress & Roth, 1971) indicated that they were usually 30–50 nm thick. The relative intensities of the reflexions lie in the approximate order $I(002) > I(003) \simeq I(005) \simeq I(007) \simeq I(004) > I(001) > I(006)$.

(i) *Pure ionic form factors*

Fig. 3 shows the results of one-dimensional systematics calculations of diffracted beam intensity as a function of crystal thickness for 00*l* reflexions with $|l| \leq 7$ in $W_4Nb_{26}O_{77}$. For neutral atoms [Fig. 3(*a*)] the relative intensities at thicknesses up to about 50 nm were similar to those found experimentally. In particular, the 001 reflexion was very weak and the 006 intensity was almost zero. For fully ionized atoms [Fig. 3(*b*)] on the other hand, the intensities oscillated with thickness much more rapidly than was observed experimentally.

(ii) *Ionicity*

For $W_4^{+1.4}Nb_{26}^{+1.8}O_{77}^{-0.7}$ [Fig. 3(*c*)], the oscillations with thickness were less rapid, but the 001 intensity was too high, being greater than that of 004, and approximately equal to 003 and 005. Even for $W_4^{+0.8}Nb_{26}^{+1.0}O_{77}^{-0.4}$ [Fig. 3(*d*)], the intensities of 001 and 004 were about equal.

11-beam 00*l* lattice fringes calculated for the above ionizations showed that the greater the degree of ionization, the greater the variation of the fringe profile with increasing crystal thickness. The images in Fig. 4 were calculated for a defect of focus of −40 nm; for comparison, images of the projected charge densities, calculated for 11 Fourier coefficients are also shown. The figure shows that this restricted-aperture projected charge density of the structure matches the image contrast at the thin edge of the wedge, the CS-planes imaging as black lines. The images of the thicker areas of the wedge exhibited a strong dependence on the degree of ionization. Experimental micrographs of wedge-shaped crystal fragments, for instance Allpress & Sanders (1971), showed little variation of fringe profile with crystal thicknesses up to approximately 30 nm, with a contrast reversal between 30 and 100 nm. Fig. 4 shows that, if this behaviour is to be matched, the degree of ionization must be kept low.

(iii) *Modified form factors*

Since the electron shells are neither infinitely rigid nor in a spherical environment, the scattering curves for ionized atoms in a lattice will not show the same increase to infinity at low values of $\sin\theta/\lambda$ that occurs for isolated ions of any ionicity (Fig. 1). This is borne out by the experimental observations both in imaging and diffraction. Indeed the observed intensities require that the inner points on the scattering curve should be substantially reduced. The modified points (Fig. 5) are found to lie approximately on straight lines through the positions appropriate for the 002 and 003 reflexions ($\sin\theta/\lambda \simeq 0{\cdot}4$, $0{\cdot}6$ nm^{-1} respectively). The shape of the form factor which results, when interpreted in terms of charge density, extends the electron cloud round the ions so that overlap with neighbouring distributions

Table 1. *Structure amplitudes for models of* $W_4Nb_{26}O_{77}$

Atom*	Degree of ionization (electrons)							
Type	Pure ionic					Modified		
W_t	0·0	6·0	1·4	0·8	0·8	6·0	1·4	0·8
W_o	0·0	6·0	1·4	0·8	1·0	6·0	1·4	0·8
Nb	0·0	5·0	1·8	1·0	1·0	5·0	1·8	1·0
O	0·0	−2·0	−0·7	−0·4	−0·4	−2·0	−0·7	−0·4
Reflexion	Structure amplitude (Volt)							
001	0·17	4·20	0·92	0·61	0·61	1·61	0·44	0·31
002	−0·66	−3·50	−1·06	−0·90	−0·89	−3·40	−1·05	−0·89
003	−0·62	−1·05	−0·59	−0·61	−0·61	−1·05	−0·59	−0·61
004	0·58	0·62	0·52	0·55	0·55	0·62	0·52	0·55
005	0·91	0·92	0·86	0·88	0·89	0·92	0·86	0·88
006	0·00	−0·05	−0·00	−0·01	0·00	−0·05	−0·00	−0·01
007	−1·37	−1·99	−1·56	−1·48	−1·47	−1·99	−1·56	−1·48
008	−0·16	−0·19	−0·17	−0·17	−0·17	−0·19	−0·17	−0·17
009	0·16	0·25	0·19	0·18	0·18	0·25	0·19	0·18
0010	0·26	0·31	0·28	0·27	0·27	0·31	0·28	0·27
0011	−0·13	−0·14	−0·13	−0·13	−0·13	−0·14	−0·13	−0·13
0012	−0·36	−0·38	−0·37	−0·36	−0·36	−0·38	−0·37	−0·36
0013	0·04	0·03	0·03	0·04	0·03	0·03	0·03	0·04
0014	1·37	1·39	1·38	1·37	1·39	1·39	1·38	1·37

* W_t is the ionization of the tetrahedrally sited tungsten atoms while W_o is that of the tungsten atoms situated in octahedral sites.

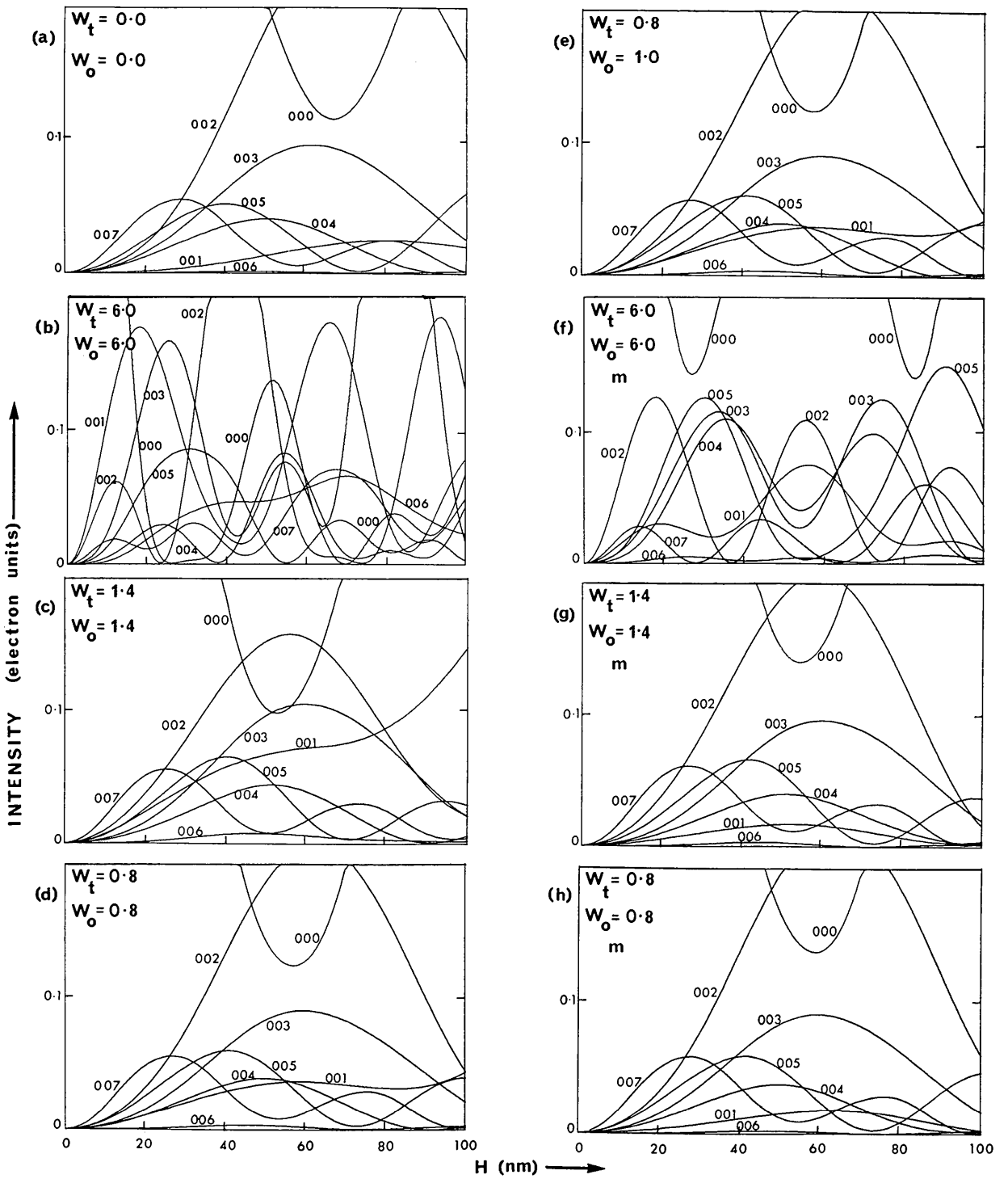

Fig. 3. Variation of *n*-beam $00l (l \lesssim 7)$ reflexion intensities, calculated for atoms having various ionizations, with crystal thickness. W_t is the ionization of the tetrahedrally sited tungsten atoms while W_o is that of the tungsten atoms situated in octahedral sites. (*a*) $W_4Nb_{26}O_{77}$ (neutral atoms); (*b*) $W_4^{6+}Nb_{26}^{5+}O_{77}^{2-}$ (fully ionized atoms); (*c*) $W_4^{1\cdot4+}Nb_{26}^{1\cdot8+}O_{77}^{0\cdot7-}$; (*d*) $W_2^{0\cdot8+}Nb_{26}^{1\cdot0+}O_{77}^{0\cdot4-}$; (*e*) $W_2^{0\cdot8+}W_2^{1\cdot0+}Nb_{26}^{1\cdot0+}O_{77}^{0\cdot4-}$ (Note that the octahedrally sited tungsten atoms carry the same charge (1·0+) as the octahedrally sited niobium atoms, while the ionization of the tetrahedrally sited tungsten atoms is 0·8+); (*f*) $W_4^{6+}Nb_{26}^{5+}O_{77}^{2-}$ (modified-atom scattering factors); (*g*) $W_4^{1\cdot4+}Nb_{26}^{1\cdot8+}O_{77}^{0\cdot7-}$ (modified atom scattering factors); (*h*) $W_4^{0\cdot8+}Nb_{26}^{1\cdot0+}O_{77}^{0\cdot4-}$ (modified atom scattering factors).

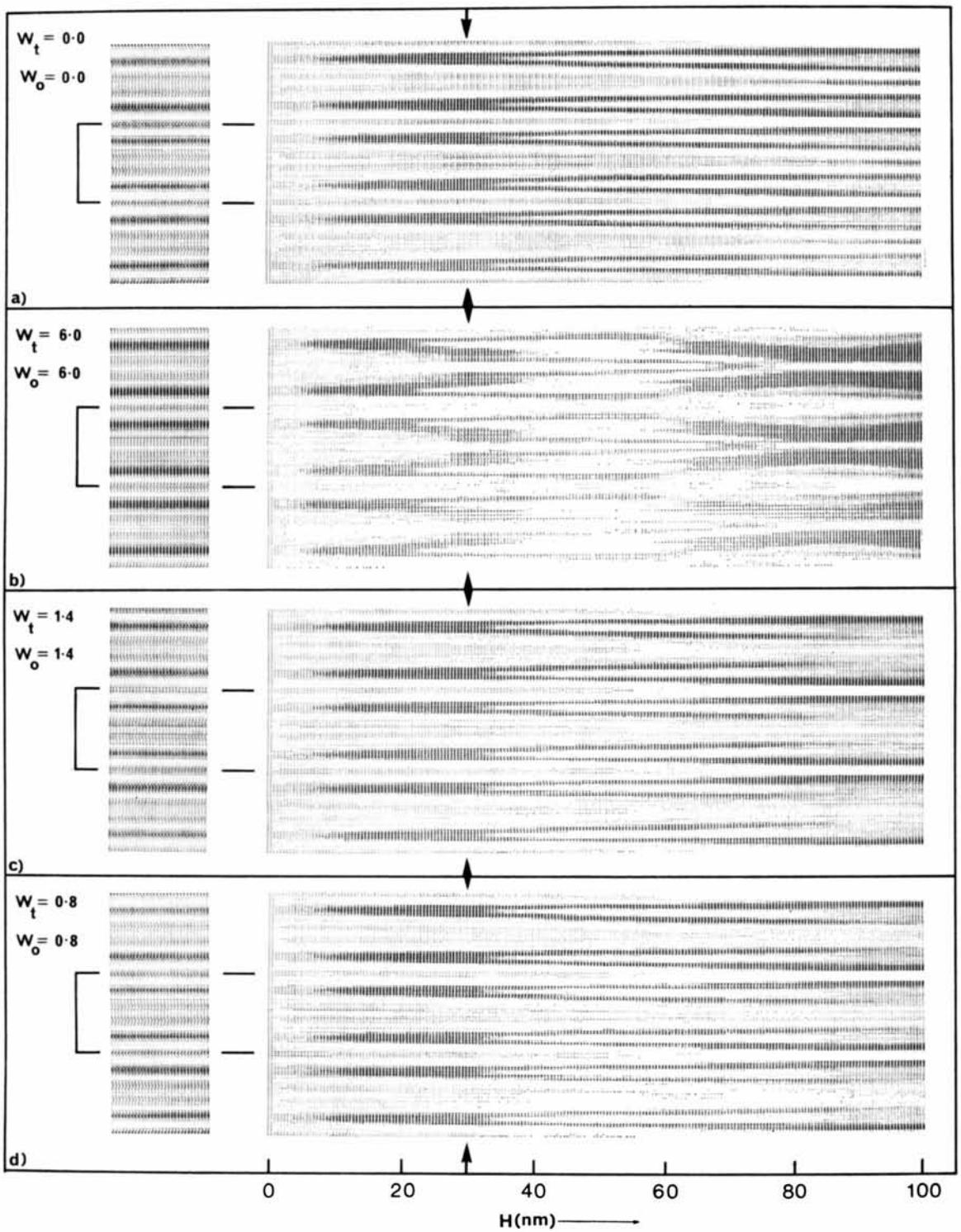

Fig. 4. Calculated wedge-crystal images of $W_4Nb_{26}O_{77}$ [variation of 11-beam $00l$ ($|l| \lesssim 5$) images with crystal thickness up to 100 nm] for 40 nm underfocus. These images are to be compared with the images computed using the restricted-aperture charge density approximation which are shown to the left. Three unit cells of the crystal are shown; the square bracket marks off the centre unit cell. For crystals of thicknesses greater than that indicated by the arrowheads, the approximation that the underfocused image corresponds to the charge density no longer holds. For thin crystals the black lines at approximately $C/4$ and $3C/4$ are the images of the projected crystallographic shear (CS) planes which are regions of high charge density. Images are shown for: (*a*) $W_4Nb_{26}O_{77}$ (neutral atoms); (*b*) $W_4^{6+}Nb_{26}^{5+}O_{77}^{2-}$ (fully ionized atoms); (*c*) $W_4^{1\cdot4+}Nb_{26}^{1\cdot8+}O_{77}^{0\cdot7-}$; (*d*) $W_4^{0\cdot8+}Nb_{26}^{1\cdot0+}O_{77}^{0\cdot4-}$.

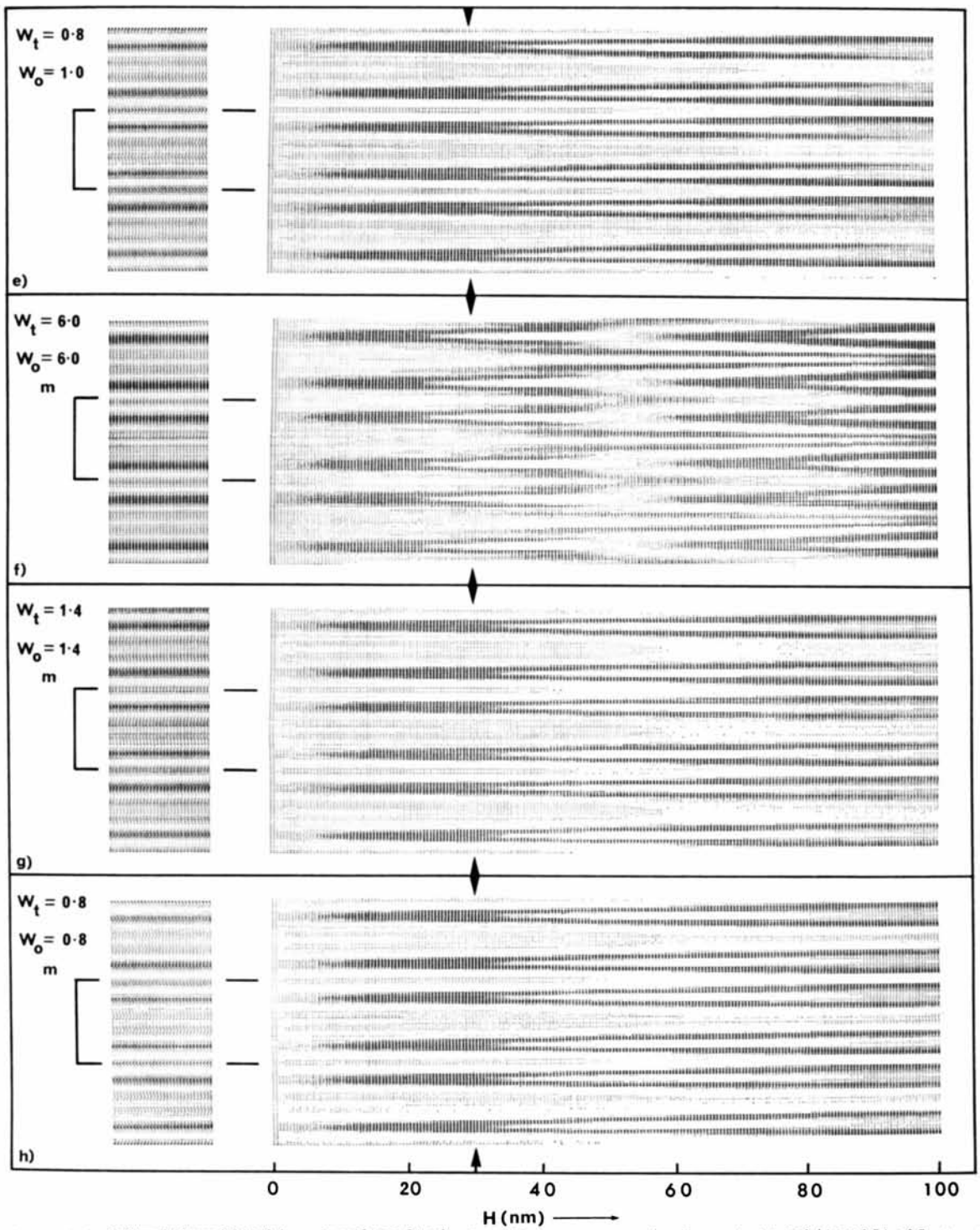

Fig. 4 (*cont.*) (*e*) $W_2^{0.8+}W_2^{1.0+}Nb_{26}^{1.0+}O_{77}^{0.4-}$; (*f*) $W_4^{6+}Nb_{26}^{5+}O_{77}^{2-}$ (modified atom scattering factors); (*g*) $W_4^{1.4+}Nb_{26}^{1.8+}O_{77}^{0.7-}$ (modified atom scattering factors); (*h*) $W_4^{1.8+}Nb_{26}^{1.0+}O_{77}^{0.4-}$ (modified atom scattering factors).

occurs; that is, covalent character is introduced into the bond. This point, along with applications of a generalized Mott formula will be described in a forthcoming publication.

Fig. 3 (*f, g, h*) shows that beam intensity *vs.* crystal thickness curves obtained for low ionization using these modified scattering factors are very like those obtained using the neutral-atom scattering factors, but

the lowest orders have a reduced quasi-period.* For example, the quasi-period of the 002 beam in 3(*a*) is approximately 150 nm, while it is only 37 nm in 3(*f*) about 150 nm in 3(*g*) and about 120 nm in 3(*h*). At the moment, our diffraction data do not allow us to distinguish between the neutral atom and partially ionized modified-ion results. Lattice images calculated using these scattering results confirm the reduced quasi-period [the quasi-period in 4(*a*) is greater than 100 nm while that of the image in 4(*f*) is 60 nm]. Diffracted beam intensities, calculated using the two-dimensional multislice technique, also showed a reduced quasi-period. The calculated two-dimensional diffraction intensities still show a lack of agreement with experiment, particularly with regard to the intensities of the off-systematic reflexions, 207, $\bar{2}07$, $\bar{2}0\bar{7}$ (Fig. 6). This may be due to errors in measurement of angle of incidence and to averaging over crystal thickness. However, the calculated images are sufficiently good to obtain good agreement with experimental images; this agreement has been displayed in Part I (Allpress *et al.*, 1972) of this series. Since it is intended to obtain more accurate diffraction data by convergent-beam techniques, it is not considered worthwhile to refine the current data further, although this would certainly be possible.

The sensitivity of the inner beams to bonding is established by the above results; the insensitivity of these beams to structure is confirmed by calculations carried out with several variations in atom positions within the unit cell and with variation of overall isotropic temperature factor.

The effect, on the inner seven 00*l* beams, of changes in atom position was examined by repeating the neutral-atom calculations with metal-atom centres moved from the final positions determined by Anderson *et al.* to those of their initial 'idealized' structure. Fig. 7(*b*) shows that these translations, of up to three times their estimated standard deviations, produced less than 2% variation in these seven 00*l* beam intensities.

Intensities calculated with values of temperature factor (B) of 0·01 nm^2 [Fig. 7(*c*)] are within 0·5% of those with $B=0$ [Fig. 7(*a*)].

* See Appendix.

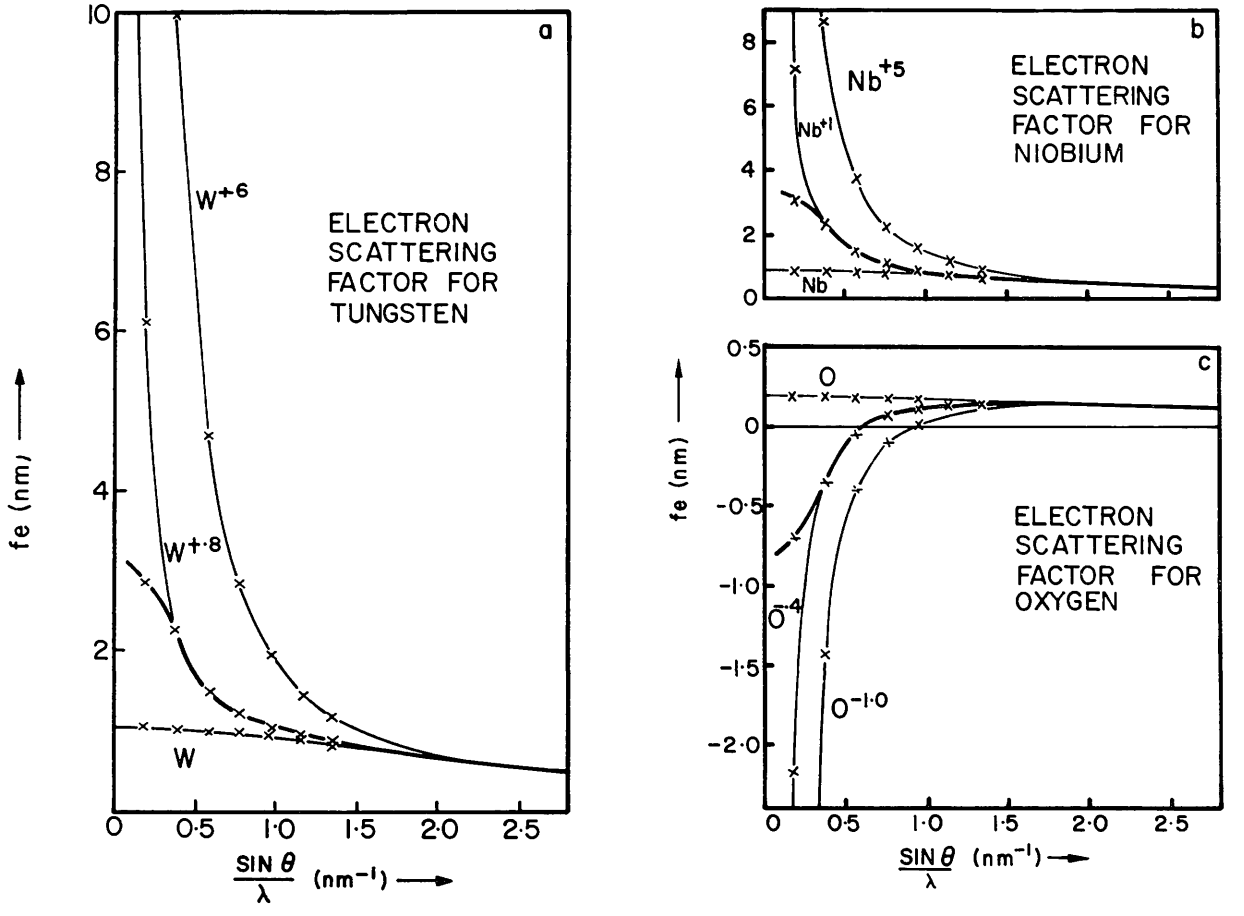

Fig. 5. Electron scattering factors for neutral and ionized atoms of tungsten (*a*), niobium (*b*) and oxygen (*c*). The modified curves (heavy lines) for partially ionized atoms ($W^{+0.8}$, $Nb^{+1.0}$ and $O^{-0.4}$) have values at the 001 position ($\sin\theta/\lambda \simeq 0{\cdot}2$ nm^{-1}) which differ from those predicted by pure ionic or ionicity models.

Discussion of results

Information on both bonding and crystal structure is therefore contained in an image of a wedge-shaped crystal. At the edges, the projected charge density of the structure is imaged, while the dependence of the image on thickness reflects the types of bonding in the crystal. Roughly, rapid changes in the image with thickness indicate pure ionic bonding in one or more atomic species, whereas relatively slow changes (as in the current investigation) indicate that all species are either largely screened or are covalently bonded. Complete calculations are necessary in order to extract quantitative information on this latter point, and for the most accurate measurements, diffraction data, particularly convergent-beam diffraction data, are required (Goodman & Lehmpfuhl, 1967), but direct images provide an immediate and powerful source of information on bonding.

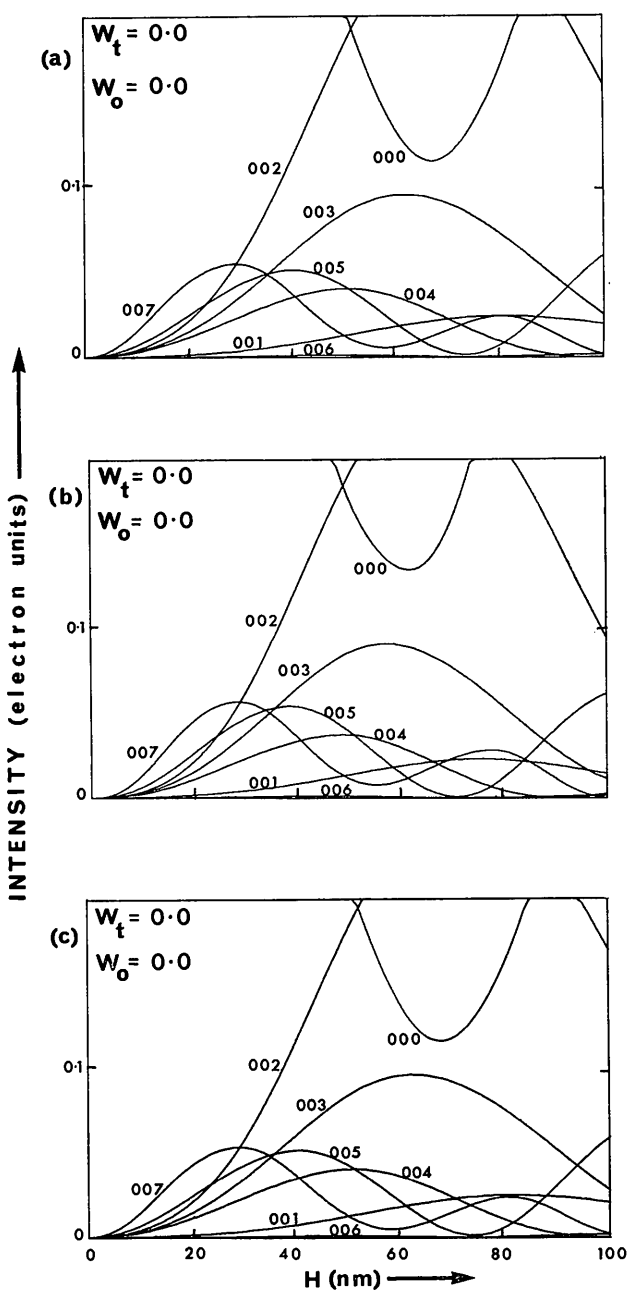

Fig. 7. Variation of *n*-beam 00*l* ($\lesssim 7$) $W_4Nb_{26}O_{77}$ reflexion intensities calculated for neutral atoms. (*a*) Temperature factor (*B*) zero; atom positions as determined by Andersson, Mumme & Wadsley (1960). (*b*) Atom positions of 'idealized structure' of Andersson *et al.* (1960); $B=0$. (*c*) Atom positions determined by Andersson, Mumme & Wadsley (1960); $B=0{\cdot}01$ nm^2.

Some qualitative points may be noted. At the large spacings (>2 nm) encountered in the current measurements, the intensities of the inner reflexions are only weak functions of atomic position, so that quite accurate information on bonding may be obtained with approximate structures. For a range of structures of increasing unit-cell edge, as the scattering angle decreases dependence on bonding increases, but the number of atomic positions in which error may accumulate due to differences in the environments of atoms increases. It might therefore be considered that this accumulation of errors would 'average' bonding effects, but bonding effects cannot be averaged to zero in dynamical scattering. The authors are indebted to Mr P. Goodman for the remark that, in the limit for small scattering angle, the mean inner potential is at once extremely sensitive to bonding and totally independent of structure. This is the limit which produces the dominating effect in large structures. The error in intuitive arguments tends to arise from misplaced analogies with X-ray refinement.

Some structures are more favourable than others for the extraction of bonding information. The current structure, which is favourable, illustrates the point. The unit-cell axes are not aligned with the main structural features, so that, kinematically, the first orders are weak, Since a first order, in dynamical scattering, couples strongly into a large range of orders, a weak first order does not swamp variation in intensity between adjacent orders and hence sensitivity to scattering factors and bonding is assured. This can readily be seen from a scattering-diagram analysis (Gjønnes & Moodie, 1965).

Conclusions

In conjunction with dynamic electron-diffraction data, lattice images provide a great deal of information on both crystal structure and bonding in structures which have large unit cells; the projected-charge-density interpretation of images of thin crystals at small defects of focus serves as a guide to interpretations of the structure, while the behaviour of the images with increasing thickness reflects the type of bonding in the crystal; relatively slow changes (as in the current investigation) indicate largely covalent bonding and rapid changes indicate ionic bonding. However, in other

cases, the rate of change of image with crystal thickness should be used only as an indication of the type of bonding present until a full calculation is carried out, since the rate of change will depend also on crystal orientation, resolution and type of structure. In this particular structure:

(1) comparison of the above calculations with experimental results shows that the atoms in $W_4Nb_{26}O_{77}$ are not fully ionized. In fact, a reasonably good match of through-focus series of experimental images was obtained using neutral-atom form factors in the calculations for the computed images (Allpress, Hewat, Moodie & Sanders, 1972);
(2) calculations carried out with values of ionization of $W_4^{+1\pm0.5}Nb_{26}^{+1.2\pm0.5}O_{77}^{-0.8\pm0.5}$, where the limits are estimates based on the computed results, can be made to match the experimental data only if a covalent character is imposed on the bonding by modifying the form-factor curves;
(3) it is of interest that Lines (1970) has obtained values of ionicity in $LiNbO_3$ by statistical mechanical arguments, of $Nb^{+1.4}$ and $O^{-0.8}$. These values lie within the range of our estimated ionicities for Nb and O;
(4) the results obtained are in accord with the deduction of Wadsley (1967), who concluded that a high proportion of covalent bonding is present in this type of structure, since the most stable arrangement of octahedra is that in which they share the maximum number of edges and faces, bringing metal atoms into close proximity.

We wish to thank Mr J. G. Allpress and Dr J. V. Sanders, who obtained the experimental results, for permission to use these results, and for helpful criticism of the manuscript.

APPENDIX

The two-beam approximation to electron scattering gives a solution which is periodic with crystal thickness. The simple relationship between the diffraction plane and the image plane ensures that the image is also periodic. This also applies to those symmetric configurations which are exactly reducible to two-beam form (Niehrs, 1958). A particularly simple example is afforded by the symmetric three-beam case.

Some many-beam configurations approach reducible configurations and it is these which we describe as quasi-periodic. This quasi-periodicity can be seen most clearly in the image of Fig. 4(*f*) and in the diffraction intensities of Fig. 3(*f*).

Approximately reducible situations may be examined by applying Zassenhaus's theorem (as quoted by Magnus, 1954) to Sturkey's (1962) solution for fast electron scattering without upper-layer-line interaction,

$$\mathbf{U}=\exp\{i\mathsf{M}z\}\cdot a_0 .$$

Here $\mathbf{U}$ is the column vector of the scattered amplitudes, M is the matrix

$$a_{ii}=2\pi\zeta_i , \quad a_{ij}=\sigma V_{i-j}$$

where these terms are defined in parts I and II; z is the coordinate normal to the entrance face of the crystal and a_0 is the column vector

$$\begin{pmatrix}1\\0\\0\\0\\\cdot\\\cdot\\\cdot\end{pmatrix} .$$

(Note that $\exp\{i\mathsf{M}z\}$ is not, of course, periodic in z for arbitrary M.)

A restricted form of Zassenhaus's theorem, sufficient for present purposes, states that for square matrices A, B of degree n there must exist uniquely determined Lie elements C_m, $(m=2,3,4,\ldots)$ which are exactly of degree m in A, B such that, $\exp\{i(\mathsf{A}+\mathsf{B})z\}=\exp\{i\mathsf{A}z\}\cdot\exp\{i\mathsf{B}z\}\cdot\exp\{iz)^2\mathsf{C}_2\}\ldots.\exp\{(iz)^m\mathsf{C}_m\}\ldots.$

Suppose that the matrix A describes a scattering configuration which is reducible and hence has a solution $U_1(z)=P(z)\cdot a_0$ periodic in z, that this configuration is perturbed, for instance by the inclusion of more beams, or by a change in angle of incidence, and that this perturbation is represented by a matrix B. Then,

$$\begin{aligned}\mathbf{U}&=\exp\{i(\mathsf{A}+\mathsf{B})z\}a_0\\&=\exp\{i\mathsf{A}z\}\cdot\exp\{i\mathsf{B}z\}\cdot\exp\{-\tfrac{1}{2}(iz)^2[\mathsf{A},\mathsf{B}]\}\cdot\\&\quad\exp\{(iz)^3\mathsf{C}_3\}\ldots a_0\end{aligned}$$

where $[\mathsf{A},\mathsf{B}]=\mathsf{AB}-\mathsf{BA}$

Suppose B is small so that the solution is approximated by a few terms in the infinite product series, and that the perturbation arises from a change in the angle of incidence, leading to changes in the excitation errors of $\Delta\zeta_i$. Then, $\mathsf{A}=\mathsf{A}$ and B is the diagonal matrix $b_{ii}=2\pi\Delta\zeta_i$.

If only the first two terms are included,

$$\mathbf{U}=\exp\{i\mathsf{A}z\}\cdot\begin{pmatrix}\cdot&&&&\\&\cdot&&&\\&&\exp\{2\pi i\Delta\zeta_i z\}&&\\&&&\cdot&\\&&&&\cdot\end{pmatrix}\cdot a_0=\mathbf{U}_1 .$$

that is, in first order, the solution remains periodic in z. The exponent, $(iz)^2\mathsf{C}_2$, in the second-order term is

$$c_{ii}=0 , \quad c_{ij}=-{}^{1}/_{2}(iz)^2\{2\pi\sigma V_{i-j}(\Delta\zeta_j-\Delta\zeta_i)\} .$$

The elements of the exponential of this real antisymmetric matrix can be evaluated as the components of the Fourier transform of the exponential of a certain antisymmetric function of the structure amplitudes and excitation errors. Details will be given in a forthcoming publication. These elements, d_{ij} say, are non-periodic

in z and, within the appropriate thickness range, constitute a non-periodic perturbation on the periodic untilted configuration.

Explicitly,

$$\mathbf{U}=\exp\{i\mathsf{A}z\}\cdot\begin{pmatrix}\vdots\\ d_{t1}\exp\{2\pi i\Delta\zeta_t z\}\\ \vdots\end{pmatrix}.$$

Thus in second order, tilt destroys the periodicity of a reducible configuration. However, over a realizable range of thicknesses and tilts, the elements of the column vector will be small, except for d_{11}, which will be close to unity, so that the main features of the periodicity will remain, giving rise to the 'quasi-periodicity' referred to in the text.

Suppose now that the perturbation arises from the inclusion of beams additional to those in the reducible configuration.

Then,

$$\mathsf{A}=\left(\begin{array}{c|c}\mathsf{A} & 0\\ \hline 0 & 0\end{array}\right),\qquad \mathsf{B}=\left(\begin{array}{c|c}0 & b_1\\ \hline b_2 & b_3\end{array}\right),$$

$$\exp\{i\mathsf{A}z\}=\left(\begin{array}{c|c}\exp\{i\mathsf{A}z\} & 0\\ \hline 0 & \mathsf{E}\end{array}\right)\quad\text{where}\quad\mathsf{E}=\begin{pmatrix}\cdot & & \\ & 1 & \\ & & 1\\ & & & \ddots\end{pmatrix},$$

and $\exp\{i\mathsf{B}z\}$ is non-periodic. Thus, the inclusion of additional beams destroys periodicity in first order. If the additional beams have, in a suitable sense, small structure amplitudes or large excitation errors, the perturbation can be sufficiently small so that quasi-periods exist, though necessarily over a restricted range of thickness.

The elements in A will in general refer to low-order reflexions and, therefore, will be heavily affected by ionicity. Increasing the weight of these elements will increase the effective structure amplitudes in the equivalent reducible case and hence reduce the period, and the overall quasi-period.

The approach to 2-beam scattering has been investigated by Goodman (1968).

Cases which include upper-layer-line interactions can be investigated with the aid of the degenerate forms of the Vandermonde determinant of the excitation errors (Moodie, 1972).

References

ALLPRESS, J. G., HEWAT, E., MOODIE, A. F. & SANDERS, J. V. (1972). *Acta Cryst.* A**28**, 528–536.

ALLPRESS, J. G. & ROTH, R. S. (1971). *J. Solid State Chem.* **3**, 209–216.

ALLPRESS, J. G. & SANDERS, J. V. (1971). In *Proceedings of the Fifth International Materials Symposium*, Berkeley, California.

ALLPRESS, J. G., SANDERS, J. V. & WADSLEY, A. D. (1969). *Acta Cryst.* B**25**, 1156–1164.

ANDERSSON, S., MUMME, W. G. & WADSLEY, A. D. (1966). *Acta Cryst.* **21**, 802–808.

COWLEY, J. M. (1953). *Acta Cryst.* **6**, 516–521.

COWLEY, J. M. & MOODIE, A. F. (1957). *Acta Cryst.* **10**, 609–619.

COWLEY, J. M. & MOODIE, A. F. (1959). *Acta Cryst.* **12**, 360–367.

COWLEY, J. M. & MOODIE, A. F. (1960). *Proc. Phys. Soc.* **76**, 378–384.

CROMER, D. T. & WABER, J. T. (1965). *Acta Cryst.* **18**, 104–109.

GJØNNES, J. & MOODIE, A. F. (1965). *Acta Cryst.* **19**, 65–67.

GOODMAN, P. (1968). *Acta Cryst.* A**24**, 400–402.

GOODMAN, P. & LEHMPFUHL, G. (1967). *Acta Cryst.* **22**, 14–24.

LINES, M. E. (1970). *J. Phys. Soc. Japan*, **28**, Supplement. (Proc. of the Second Int. Meeting on Ferroelectricity 1967), 175–177.

LYNCH, D. F. & O'KEEFE, M. A. (1972). *Acta Cryst.* A**28**, 536–548.

MAGNUS, W. (1954). *Commun. Pure Appl. Math.* **7**, 649–673.

MOODIE, A. F. (1972). *Z. Naturforsch.* **27a**, 437–440.

NIEHRS, A. (1958). *Fourth Int. Conf. Electron Microsc. Berl.* **1**, 316.

PAULING, L. (1960). *The Nature of the Chemical Bond.* Ithaca: Cornell Univ. Press.

STURKEY, L. (1972). *Proc. Phys. Soc.* **80**, 321–354.

WADSLEY, A. D. (1967). *Helv. Chim. Acta, Werner Centenary Volume*, p. 208.